# Thermo-optical studies of asphaltene solutions: evidence for solvent–solute aggregate formation

S. Acevedo[a,*], M.A. Ranaudo[a], J.C. Pereira[a], J. Castillo[b], A. Fernández[b], P. Pérez[b], M. Caetano[b]

[a]*Laboratorio de Físico Química de Hidrocarburos, Escuela de Química, Facultad de Ciencias, Universidad Central de Venezuela, Apartado 47102, Caracas, 1041, Venezuela*
[b]*Laboratorio de Espectroscopía Láser, Escuela de Química, Facultad de Ciencias, Universidad Central de Venezuela, 47102, Caracas, 1041A, Venezuela*

## Abstract

Thermo-optical diffusivities, $D$, were measured for Hamaca, Cerro Negro and Furrial asphaltenes in both toluene and tetrahydrofuran. In toluene a plot of $D$ vs. log $c$ where $c$ was the asphaltene concentration, afforded an unexpected minimum near 50 mg $l^{-1}$. Similar plots in THF for Hamaca asphaltenes yielded the result with little or no change in $D$ with concentration changes. The reduction in $D$ before the minimum ($c < 50$ mg $l^{-1}$ in toluene) is consistent with the trapping of a layer of solvent between solute molecules (sort of solute–solvent aggregates) presumably resulting in a higher heat capacity for the solvent in this aggregate when it is compared with the solvent in the bulk. At higher concentrations, and probably because of the collapse of the solute–solvent aggregates and the formation of solute–solute aggregates (dimers, trimers, etc.), solvent is released to the bulk, leading to increases in $D$ until a fairly constant value is reached near 2000 mg $l^{-1}$. © 1999 Elsevier Science Ltd. All rights reserved.

*Keywords:* Asphaltenes; Thermo-optical diffusivity; Solute–solvent aggregates

## 1. Introduction

The molecular interaction in asphaltenes is an important and interesting feature of these materials as it is related to phenomena such as aggregate and flock formation, low solubility and asphaltene flocculation. Naturally, interaction studies have been focused on asphaltene–asphaltene or solute–solute interaction rather than solute–solvent interactions. However, studies on solute–solvent interactions, particularly with aromatic solvents such as toluene, could give important information regarding the concentration at which the aggregation begins and the possible interaction of asphaltene with other crude oil components such as resins and aromatics. As is the case for any associative solute, desolvation should occur before aggregation, and the extent and the way of this desolvation could give important clues regarding the solute–solvent affinity. For instance, in micelle formation in water with ordinary surfactants, desolvation of carbon chains occurs quite sharply at the cmc which is due to the 'hydrophobic effect' [1]. That is, the affinity of water for itself is too large compared to the one for hydrocarbons. Hence, the main driving force for micelle formation is water desolvation rather than solute–solute interactions and, consequently, no water is found within the hydrocarbon core of micelles [1].

It is a very well-known fact that in an oil medium, micelle formation occurs by mechanism unrelated to the one in water [2,3]. For instance, among the differences, no cmc is found, the number of aggregation is much lower and some oil may be trapped within the aggregates. A complete discussion on this topic has been given by Kertes [3]. In an oil medium [2,3] and in particular, for the asphaltene case where dimers, trimers and higher aggregates are formed as the concentration is increased, a stepwise mechanism, is more likely. Probably, the reason for this is that both the asphaltene and the media are 'oily' in nature and thus a significant energy barrier for desolvation might be present. Hence a process whereby desolvation occurs as a phase separation (such as the micelle formation at the cmc) is unlikely.

As suggested by the evidence discussed later, solvent molecules are trapped during asphaltene aggregation. If this behavior is extrapolated to the aggregates in crude oil, then, besides asphaltenes they should contain a variety of compounds, such as resins and aromatics. This, of course, would have very important consequences in asphaltene solubility.

* Corresponding author. Fax: + 58-02-605-22-46.
*E-mail address:* soaceved@strix.ciens.ucv.ve (S. Acevedo)

Table 1
Properties of materials used

| Sample | API[a] | %[b] | H/C[c] | $f_a^d$ |
|---|---|---|---|---|
| Hamaca asphaltene[e] | 9 | 12 | 1.13 | 45 |
| Cerro Negro asphaltenes[e] | 8.3 | 13 | 1.14 | 50 |
| Hamaca resins[e] | — | 9 | 1.38 | 22 |
| Furrial asphaltenes | 21 | 10 | 0.97[f] | 56[g] |

[a] Of crude oil.

[b] Respect to crude oil.

[c] Hydrogen to carbon ratio.

[d] Aromaticity (% of aromatic carbons).

[e] From Ref. [5].

[f] From Ref. [11].

[g] Obtained by NMR as usual.

In view of the well-known capacity of asphaltenes to aggregate, their study, particularly, in non-polar solvents requires the examination of highly diluted solutions (less than say 50 mg l$^{-1}$). Hence, a very sensitive and specific technique should be used. In this study we measured the thermal diffusivities, $D$, by means of a thermal lens spectroscopy (TLS) technique [4] to investigate the behavior of asphaltene solutions in toluene and tetrahydrofuran (THF). Using this method, it is possible to investigate solutions below 1 mg l$^{-1}$ without difficulties. What is actually measured is the characteristic time $t_c$ and from this $D$ is calculated. As it is a property of the solvent, it should be independent of the solute.

However, as discussed later, asphaltenes change the local properties of the solvent that surround it, and (somewhat unexpectedly) $D$ is one of them.

## 2. Experimental

Asphaltenes were obtained from crude oil as described earlier [5]. Extraheavy Hamaca and Cerro Negro crude oil was diluted with toluene (1:1 (v/v)) before the addition of $n$-heptane (40 v). Medium Furrial oil was treated directly with
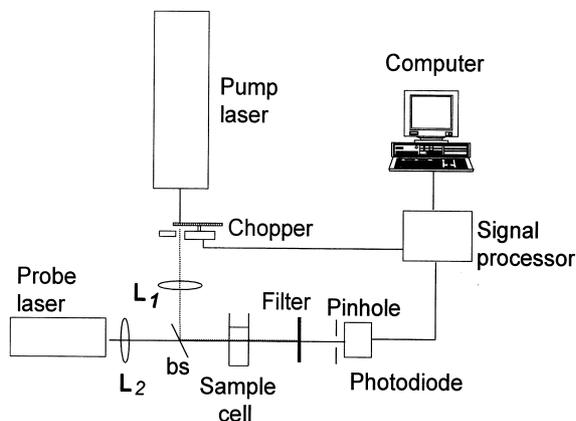


Fig. 1. Schematic representation of a dual beam thermal lens spectrometer system. $L_1$ and $L_2$ are convergent lenses, (b.s.) beam splitter and (o.d.) neutral density optical filter.
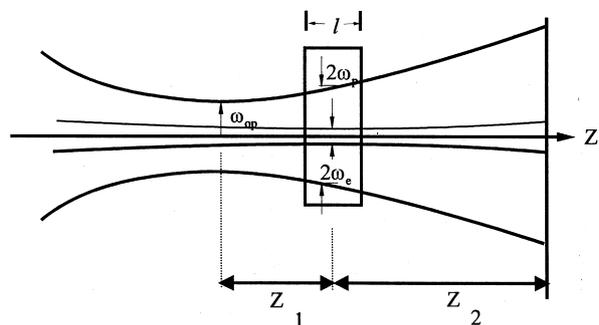


Fig. 2. Schematic diagram of a dual-beam mismatched thermal lens optical configuration. $\omega_p$ and $\omega_e$ are the radius of the probe and excitation beam at cell center; $\omega_{op}$ is the radius of the probe beam at its focus; $Z_1$ is the distance from the center of the sample to the waist of the probe beam; $Z_2$ is the distance from the center of the sample to the aperture diameter and $l$ is the sample cell lenght.

$n$-heptane (40 v). In both cases the precipitated resins were removed by Soxhlet extraction with boiling $n$-heptane. Solutions of desired concentration, were prepared by dilution as usual and measurements were performed after a three-day period to minimize aging problems. Some properties of the asphaltenes and resins studied are shown in Table 1.

### 2.1. Instrumental

#### 2.1.1. Optics

The thermal lens spectrometer was based on a collinear dual-beam configuration. A schematic diagram of the apparatus is shown in Fig. 1. A Coherent Innova 300 argon ion laser (514.5 nm) was used as a pump beam. The excitation beam, which was amplitude modulated by a mechanical chopper, was focused onto the sample cell with lens $L_1$ (200-mm focal length). A 5 mW He–Ne laser (model 05-LHR-151 Melles Griot, 632.8 nm) was used as a probe beam and focused with lens $L_2$ (200-mm focal length). A 3-mm cuvette was used as the sample cell. A 50% beam splitter was used in order to direct collinearly the excitation and the probe beam through the sample cell. The transmitted excitation beam was blocked after the sample with an absorption filter. The thermal lens signal was obtained by sampling the intensity at the center of the probe beam with a precision pinhole (100 μm) and a silicon photo diode (Melles Griot LM2). The detector–pinhole system was mounted in an XY translator in order to localize the laser beam center. The photocurrent is amplified using a trans impedance amplifier (Melles Griot 13-AMP-003).

#### 2.1.2. Data processing

The amplified photo current was digitized using a personal computer with an ADC/DAC board (Lab-PC card, National Instruments). The sampling rate used was 200 samples per second. The initial intensity of probe beam $I(0)$ was taken at the beginning of each shutter pulse. The
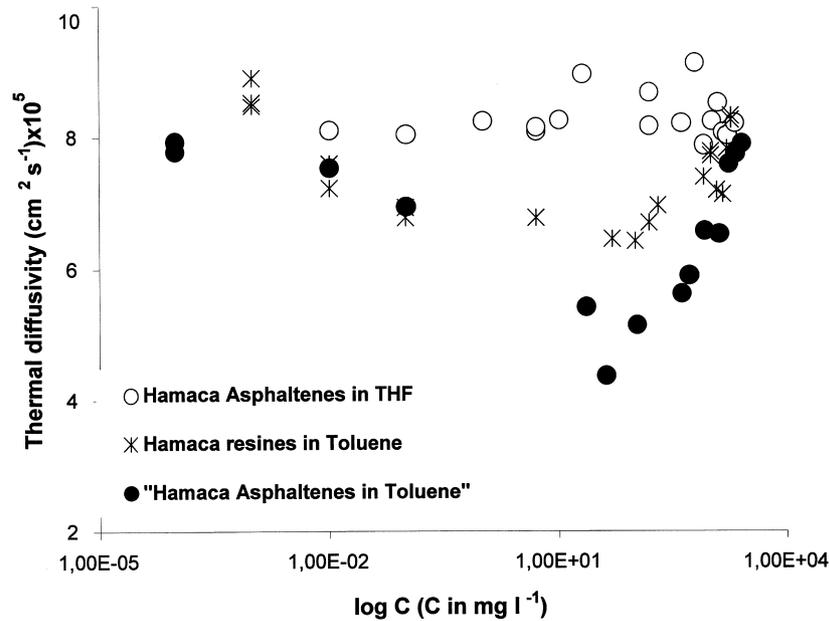
Fig. 3. Plot of thermal diffusivities $D$ (cm$^2$ s$^{-1}$) vs. log $c$, ($c$ in mg l$^{-1}$) for several sample solutions in toluene or THF at room temperature.

Levenberg–Marquardt algorithm [6] to non-linear least squares fitting was used to fit the Eq. (1) to the data.

## 3. Theory

In thermo-optical techniques, a temperature rise is produced in a sample medium by non-radiative relaxation of the absorbed energy from a modulated optical source, such as a laser beam. As the refractive index of most materials changes with temperature, this temperature rise generates a perturbation of the refractive index of sample, which acts as an optical element.

In TLS, the effect is probed as a relative change in the beam center intensity of a probe laser, passing through the center of the lens (thermal lens) induced by the excitation beam [7].

Higher sensitivities have been obtained using a dual-beam mode-mismatched thermal lens optical configuration [8]. In Fig. 2 a schematic diagram of this configuration is showed, where a TEM$_{00}$ Gaussian beam is focused in a cell containing an absorbing sample causing a thermal lens. A second TEM$_{00}$ Gaussian beam, which is collinear with the excitation beam, is incident to the sample to probe the thermal lens. The position of the probe beam waist ($\omega_{op}$) is taken as the origin along the Z-axis. A sample cell of length $l$ is located at $Z_1$ and the detector plane is positioned at distance $Z_2$ from the cell. The radii of the probe beam and the excitation beam in the cell are $\omega_p$ and $\omega_e$, respectively. Shen et al [9] have recently developed a cw laser induced thermal lens quantitative model which precisely describes the behavior of a mode-mismatched spectrometer. The time resolved signal is expressed using the equation:

$$\frac{I(t)}{I(0)_0} = \left[ 1 - \frac{\theta}{2} \tan^{-1} \right.$$

$$\left. \times \left( \frac{2m(Z_1/Z_c)}{[(1 + 2m)^2 + V^2](t_c/2t) + 1 + 2m + (Z_1/Z_c)^2} \right) \right]^2,$$

(1)

where $I(t)$ is the intensity at the center at the time $t$, $I(0)$ the value of $I(t)$ when $t$ is zero, $Z_c$ the confocal distance, and the degree of mode mismatched $m$ is given by

$$m = \left( \frac{\omega_p}{\omega_e} \right)^2$$

(2)

and $\theta$ is

$$\theta = -\left[ \frac{P_e(d\eta/dT)}{k\lambda_p} \right] A,$$

(3)

where $P_e$ is the total power of the excitation laser beam, and $\eta$ the sample refractive index, $k$ the thermal conductivity, $\lambda_p$ the wavelength of the probe beam, and $A$ the sample absorption coefficient (cm$^{-1}$). The parameter $t_c$ is a characteristic thermal time constant:

$$t_c = \frac{\omega_e^2}{4D},$$

(4)

where

$$D = k \over \rho C$$

(5)

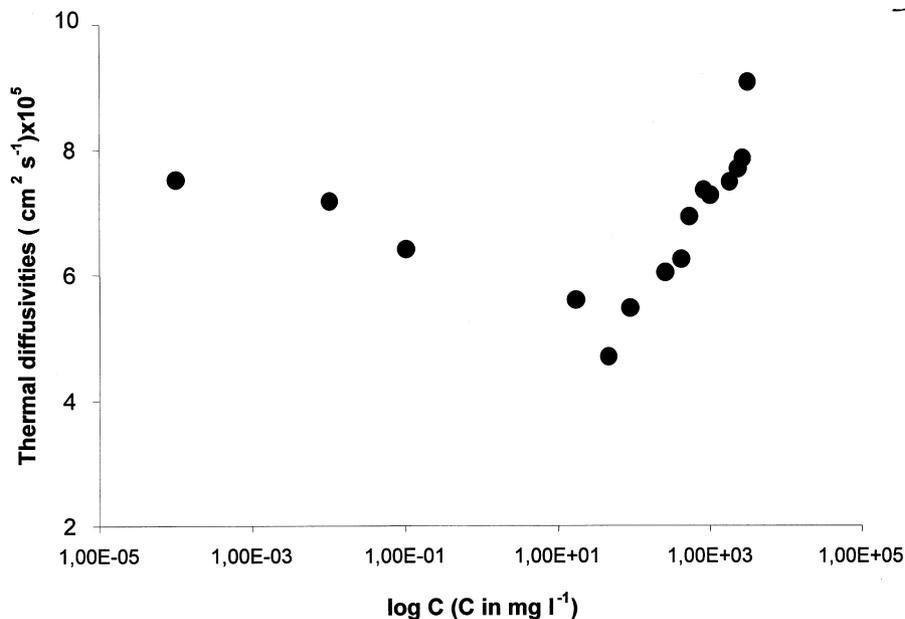is the thermal diffusivity (in cm$^2$ s$^{-1}$), $C$ and $\rho$ are the specific

Fig. 4. Plot of $D$ (cm$^2$ s$^{-1}$) vs. log $c$ ($c$ in mg l$^{-1}$) for toluene solutions of Furrial asphaltenes at room temperature.

heat ( in J g$^{-1}$ k$^{-1}$) and the density ( in g cm$^{-3}$) of the sample, respectively.

In short the experiment could be described as follows: the asphaltene in solution absorb energy from the excitation beam as usual. Through fast non-radiative relaxation of excited species, part of this energy is then transferred as thermal energy (heat) to the solvent and a density change within the excitation region is induced. The probe laser 'probes' the refractive index gradient (thermal lens) induced by the density change. The decay of the thermal lens signal, $I_t/I_o$, through dissipation of the temperature gradient by thermal diffusion, is governed by the characteristic time $t_c$. Fitting the data to the non-linear Eq. (1) allows the determination of $t_c$ from which $D$ is obtained (Eq. (4)). $D$ is the heat diffusion coefficient and conceptually is equivalent to the usual diffusion coefficient of matter.

According to its definition (Eq. (5)), $D$ depends inversely on the specific heat or the heat capacity of the solvent. This is very important as this dependence could be used to visualize the changes in $D$. For instance under conditions of constant pressure (constant $\rho$) and low concentration (constant $k$), a decrease in $D$ must be due to an increase in
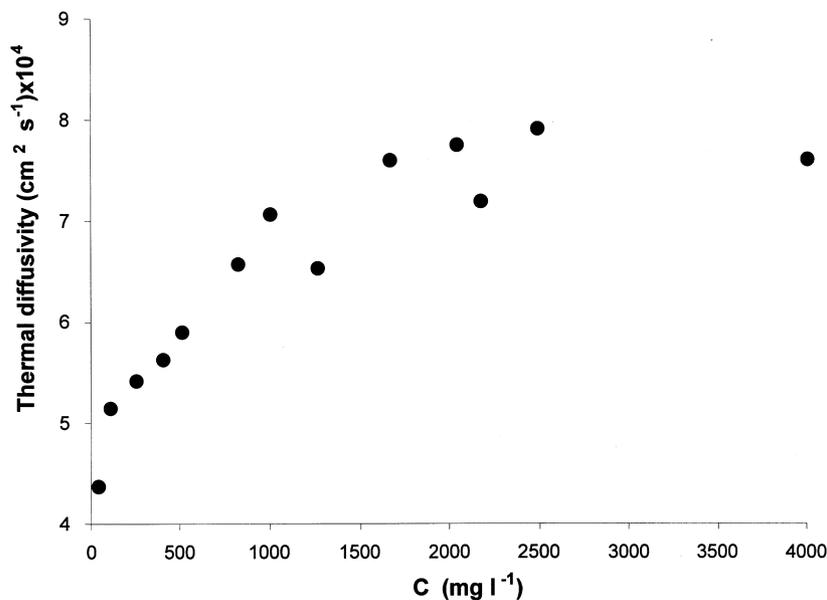


Fig. 5. Thermal diffusivity $D$ vs. concentration $c$ for solutions of Hamaca asphaltenes in toluene at room temperature. For convenience a concentration range from 41 (corresponding to $D_m$) to 4000 mg l$^{-1}$, was selected.
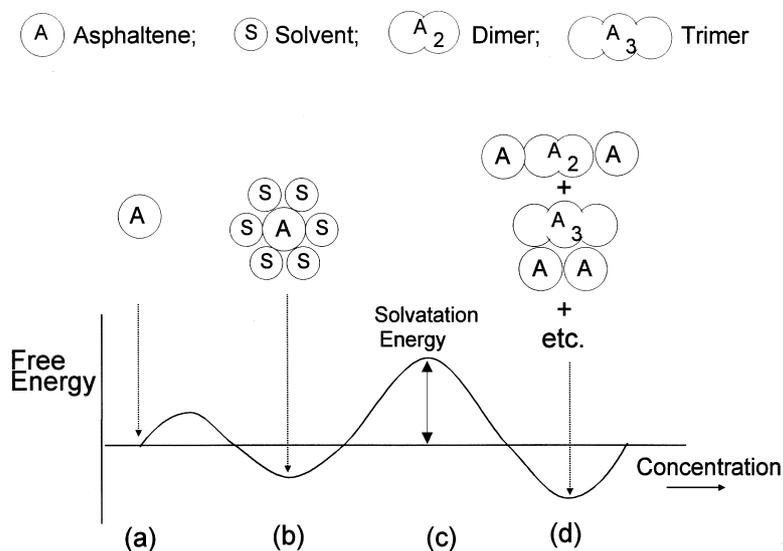
Fig. 6. Imaginary view depicting the sequence of events for asphaltene (A) solutions in toluene. Circles around A represent the layer of solvent that solvates the asphaltenes and forms a kinetic unit with it. (a) Region of high dilution with no solute–solute interactions; (b) solute–solvent aggregates. Solvent is trapped between interacting solutes; (c) free energy barrier for desolvation and aggregate formations; (d) region of moderate dilution ($\sim 2\ \mathrm{g\ l^{-1}}$).

the local heat capacity $C_{p,L}$ of the solvent, that is the solvent surrounding the solute.

## 4. Discussion and results

Plots of $D$ vs. log $c$ for the systems studied, are shown in Figs. 3 and 4 for Hamaca and Furrial samples, respectively. Results for Cerro Negro asphaltenes in toluene were very similar to the other asphaltene samples and are not shown here. When measured in toluene, curves $D_{(\log c)}$ for Hamaca, Cerro Negro and Furrial asphaltenes afforded minimum values near 50 mg $\mathrm{l^{-1}}$. After that, a continuos increase in $D$ was observed until a steady value near 2000 mg $\mathrm{l^{-1}}$ was obtained. This last feature is not clearly revealed in the above $D$–log $c$ plots. Thus a $D$–$c$ plot for the Hamaca case is shown in Fig. 5. The results are the same as that in Fig. 3 in the concentration range above 40 mg $\mathrm{l^{-1}}$, value corresponding to $D_m$, the minimum value of $D$ in this case.

A similar behavior was observed for the toluene solution of Hamaca resins (see Fig. 3), although in this case only a very shallow minimum was obtained. It is plausible that for the resin case the observed behavior is due to the presence of small amounts of asphaltene. For Hamaca asphaltenes in THF, a fairly constant $D$ value which is independent of the concentration was observed (see Fig. 3).

As the asphaltenes tend to aggregate in non-polar solvents, it is reasonable to account for these results in terms of solute interactions both with the solvent and with itself. For instance, when the number average molecular weight $M_n$ of Hamaca asphaltene and its corresponding methylated derivative were determined in benzene, values of 11 000 and 3 000 Da, respectively were obtained. It is well known that diazomethane methylation of asphaltenes

leads to lower molecular weight methylated samples [5,10]. Also it has been reported that $M_n$ values for Hamaca, measured in toluene, changes from 4230 to 17 420 over a period of two days [11].

As mentioned earlier plots of $D$ vs. log $c$ in toluene leads to a minimum which is totally unexpected. The expected result in a diluted solution is a line parallel to the concentration axis [12] similar to the one for asphaltenes in THF (Fig. 3). For toluene solutions of asphaltenes, three regimes are present in Figs. 3 and 4 suggesting the formation of different species as the total concentration is increased. The following mechanism is consistent with these results: in the first regime (negative slope, before the minimum), a significant amount of solvent molecules are used for solvating a single asphaltene molecule leading to the formation of a layer of solvent around the solute. It is expected that this solvent layer would move around with the asphaltene, forming a kinetic unit.

If the solution is ideal (no interaction between solute molecules), the amount of solvent around any solute molecule and the capacity of the solvent to diffuse heat, measured by $D$, should remain constant when solute concentration is increased. This is the expected result and is illustrated by the behavior shown by Hamaca asphaltenes in THF. However, because of high molecular weight and asphaltene interaction in toluene, a significant amount of solvent could be 'trapped' between interacting solute molecules leading to a sort of solvent–solute aggregates (see Fig. 6). Apparently, this effect increases the local heat capacity $C_{p,L}$ of the system (see the Section 3 and Eq. (5)) and consequently the thermal diffusivity is reduced leading to the observed negative slope before the minimum (see Figs. 3 and 4). An increase in the $C_{p,L}$ means that compared to the bulk

solvent, more energy could be absorbed by the solvent surrounding the solute and less would be passed on to the neighborhood.

Further increase in the concentration above $c_m$, the value corresponding to $D_m$ the minimum $D$ (second regime) eventually leads to the collapse of the solvent–solute aggregates. This in turn, leads to the formation of asphaltene aggregates (dimers, trimers, etc). As a result diffusivity increases because of the liberation of trapped solvent molecules, until a fairly constant value of $D$ is obtained (third regime, see Fig. 5).

Fig. 6 is an imaginary view of how the free energy changes with concentration (equivalent to average solute–solute distance). At low concentrations, a relatively shallow minimum should be present corresponding to the solvent–solute aggregate formation (Fig. 6(b)). At higher concentrations a deeper minimum, corresponding to aggregate formation should also be present (Fig. 6(d)). The barrier between the two (Fig. 6(c)) allows for the 'desolvation energy' needed for solvent liberation.

Irrespective of the mechanism suggested to account for the diffusivity decrease, aggregation of asphaltene in toluene appears to begin at an extremely low concentration. Apparently, aggregation begins near 50 mg l$^{-1}$ and continues up to about 2000 mg l$^{-1}$ where a plateau is reached (see Fig. 5). To have an idea of the changes in the chemical potential, if the process were micelle formation at the cmc, the following procedure can be considered.

In doing so any dimer, trimer and so on are bypassed or neglected. Then the aggregate, at the molar fraction $X_n$, should be in equilibrium with single molecules of molar fraction $X_s$. The corresponding change in standard chemical potential of transfer of asphaltene from toluene to the aggregate, per mole of asphaltene $\Delta G°$ would be:

$$\Delta G° = -(1/n)RT\ln(X_n/X_s^n) \tag{6}$$

and

$$\Delta G° = -(1/n)RT \ln X_n + RT \ln X_s, \tag{7}$$

where any effects due to activity coefficients have been neglected.

For any value of $n$ larger than say, 10, the first term could be neglected and:

$$\Delta G° \approx RT \ln X_s. \tag{8}$$

In this case, and taking the asphaltene molecular weight to be equal to 2000 Da, a $\Delta G° \approx -7$ kcal mol$^{-1}$ could be estimated for a concentration near the minimum concentration ($\approx$50 mg l$^{-1}$). This value is close to the one obtained for the solubility of hydrocarbons in water [1]. If it were close to the actual one, it would mean that the affinity of asphaltenes for toluene is extremely low.

Of course, the above treatment is identical to the micelle formation at the cmc and is not applicable in the present case. This is so because above $D_m$, $D$ increases continuously in a very wide range of concentrations. Recently, sudden changes in $D$ at the cmc were reported for surfactants in water [12]. Naturally, this is the expected behavior in water.

A better approach would be to consider the step by step formation of solute aggregates. That is, when increasing the concentration above $X_s$ or $c_m$ a continuous rather than a sharp decrease in free energy should be expected.

It is important to realize, that the way asphaltenes aggregate should be related to its affinity to the media. For instance, a step-wise aggregation where toluene gets trapped to some extent, suggests an important lyophilicity in the pair asphaltene–toluene.

Accordingly, as mentioned earlier, aggregates in crude oil should contain asphaltenes and a complex mixture of resins, aromatics and other crude components. Previously SARA mixtures (saturated, aromatics, resins and asphaltenes) have been found in precipitated asphaltenes, both from crude oil and from organic solids sampled from production facilities [13,14].

The aforementioned arguments suggest that aggregates and flocks in crude oil should be relatively easy to break apart which obviously is the case as they are highly soluble in aromatics. This high solubility, should be due to the variety of different compounds present in the aggregate, rather than to a 'peptizing' or interfacial effect of resins. For instance, it has been demonstrated that asphaltene solubility in toluene decreases from 10% (w/v) to practically zero, when 15% of the sample is removed by a mixture of THF–acetone [13].

## 5. Conclusions

Use of the thermo-optic technique allows the study of very diluted ($10^{-4}$ to 100 mg l$^{-1}$) and more concentrated (100–2000 mg l$^{-1}$) asphaltene solutions. Plots of thermal diffusivity $D$ against concentration in toluene yielded a minimum. The reduction in diffusivity measured under these conditions in toluene (concentration $< 100$ mg l$^{-1}$) could be due to the trapping of solvent molecules in solvent–solute aggregates. Presumably, such trapping decreases the capacity of the solvent to diffuse heat, as measured by $D$. At higher concentrations beyond the minimum, the continuous increase in $D$ in a wide concentration interval, appears to be consistent with a step-wise formation of dimers, trimers, etc.

# References

[1] Tanford C. The hydrophobic effect. Formation of micelles and biological membranes. 2. New York: Wiley, 1980, Chapters 1–7.

[2] Hiemenz PC. Principles of colloid and surface chemistry. 2. New York: Marcel Dekker, 1986 p. 463.

[3] Kertes AS, Gutman H. In: Matijevic E, editor. Surface and colloid science, 8. New York: Wiley, 1976.

[4] Dovichi NJ. CRC Crit. Rev Anal Chem 1987;17:357.

[5] Acevedo S, Mendez B, Rojas A, Layrisse I, Rivas H. Fuel 1985;64:1741.

[6] Numerical recipes in Fortran 77. The art of scietific computing, 2. Cambridge: Cambridge University Press, 1992.

[7] Fang HL, Swofford RL. In: Kliger DS, editor. Ultrasensitive laser spectroscopy, New York: Academic Press, 1983. pp. 176.

[8] Snook RD, Lowe RD. Analyst 1995;120:2051.

[9] Shen J, Lowe RD, Snook RD. Chemical Physics 1992;165:385.

[10] Ignasiak T, Kemp-Jones AV, Strausz OP. J Org Chem 1977;42:312.

[11] Acevedo S, Castillo J, Fernandez A, Goncalves S, Ranaudo MA. Energy and Fuel 1997;17:368.

[12] Castillo J, Fernández A, Mujica V. Mikro Chimica Acta 1998;130:105.

[13] Acevedo S, Escobar G, Ranaudo MA, Piñate J, Amorín A, Díaz M, Silva P. Energy and Fuels 1997;11:774.

[14] Acevedo S, Ranaudo M A, Escobar G, Gutierrez LB, Gutierrez X. ch. IV. In: Sheu EY, Mullins O, editors. Asphaltenes: fundamental and applications, New York: Plenum Press, 1995. pp. 131.